International Journal of Applied Engineering Research ISSN 0973-4562 Volume 14, Number 7 (2019) pp. 1527-1531

Vibration Behaviour of Aluminium Foam Core Sandwich Composites subjected to Dynamic Loading

[1]Sapthagiri. G, [2]Dr. H. K. Shivanand

[1]Research Scholar, [2]Professor

[1,2] Department of Mechanical Engg., UVCE., Bangalore University, Bangalore, Karnataka, India

Abstract

Aluminium foam has a range of properties that are desirable in many applications. These properties include good stiffness and strength to weight ratios, impact energy absorption, sound damping, thermal insulation and non-combustibility. Many of these characteristics are particularly attractive for core materials within sandwich structures. The combination of aluminium foam cores with thermoplastic composite skins is easily manufactured and has good potential as a multifunctional sandwich structure useful in a range of applications. This paper has investigated the vibration behaviour of such structures using an experimental technique. The development of these structures towards commercial use requires a thorough understanding of the deformation and strain mechanisms of the structure, and this will, in turn, allow predictions of their structural behaviour in a variety of loading conditions.

Keywords: Metal Foam, Carbon Fabric, Vibration, Modal Analysis, Sandwich Composites

1. INTRODUCTION

Metal foams can be designed to exhibit lower density and higher specific properties including stiffness, energy absorption, and mechanical and acoustical damping capacities compared to fully dense material [1]. Metal matrix foams (MMFs) are a specific class of metallic foams. They incorporate porosity in their foam-like structure by means of hollow particles dispersed in a matrix [2]. Syntactic foams are often used as core materials in sandwich composites for structural components in a wide range of applications. The high specific mechanical properties and the tailor ability make them useful in weight sensitive applications [3]. Syntactic foams can provide benefits in many fields, for example in automobile and ship structures due to their light weight and high energy absorption ability under compression. A change in the filler type and content can provide the desired balance between the properties, performance and density of syntactic foams [4].

Syntactic foams show excellent properties under compressive loading conditions because particles become load bearing elements under compression [5,6]. Hollow particles of alumina (Al_2O_3), silicon carbide (SiC), boron nitride (BN), titanium oxide (TiO_2) and fly ash cenospheres have been used as reinforcements in syntactic foams [4]. Since marine and aerospace structures are continuously exposed to vibrations, the internal damping capabilities of these materials are extremely useful [7-10]. Metal matrix syntactic foams can be fabricated by different methods. The most common are the pressure or pressureless infiltration methods [11-13]. In these techniques the molten matrix infiltrates into a randomly packed preform of spheres followed by solidification under controlled conditions. Another fabrication method is the melt stirring method, where hollow particles are mixed into the matrix melt followed by solidification [11]. Aluminium matrix syntactic foams synthesized by these methods have been studied for a wide range of loading conditions and material parameters [14-16].

To enhance the mechanical properties of metallic foams, they have been sandwiched between two stiff sheets. The face-sheets (or skins) provide the material with increased tensile and flexural strength and stiffness while the foam core allows it to withstand large deformation and absorb energy [17]. Metal foams and foam core sandwich composites are promising protective materials in applications such as vehicle crumple zones and blast armors [18]. Although syntactic foams are also intended for use as core materials in sandwich structures, metal matrix syntactic foam core sandwich materials have only been studied recently because of challenges involved in their fabrication [19,20]. Studies on compression and flexural response of aluminium matrix syntactic foam core sandwich composites are available [19-22]. These studies were conducted on sandwich specimens having one layer of fabric skin on each side.

Since MMSF core sandwich composites are only recently realized, their vibration response, to the best of knowledge, has not been analysed yet despite interest in such properties for their envisioned applications. Due to their ease of implementation, vibration-based methods are advantageous over wave propagation methods for dynamic characterization [23-26]. Free vibration of a cantilever beam was used in Ref. [23] to assess the dependence of dynamic mechanical properties of syntactic foams on hollow particle filler wall thickness and volume fraction. For functionally graded beams, the effects of constituent volume fractions, volume fraction gradient, and slenderness ratios on the natural frequency have been investigated using beam theories [27]. A theory for the vibration and stability of symmetric sandwich beams with elastic bonding has been developed by Ref. [28]. The main assumption was that the interfacial bond between the face layer and the core is thin and elastic and the bond shear tractions between the layers are proportional to the relative tangential displacement of the layers at the interface. Many other works based on the theoretical prediction of the free vibration response for sandwich composite materials are available in literature [29-31]. Availability of the natural frequency and dynamic properties of metal matrix syntactic foam core sandwich material can help in designing structures that can benefit from these properties. It is also noted in most previous

studies on metal matrix syntactic foams that only the strength values are reported. The stiffness values are not reported mainly because the measured values are very low due to compliance of the test machine and other issues.

2. EXPERIMENTAL DETAILS

2.1 Material

Aluminium alloy (Al2014) were used as raw materials for manufacture of Foam Core of Sandwich Composites. The alloy nominally contains Cu: 0.7 wt.%, Mg: 1.0 wt.%, Si: 11.8 wt.%, Fe: 1.0 wt.%, Mn: 0.5 wt.%, Ni: 1.5 wt.%, Zn: 0.5 wt.%, Pb: 0.05 wt.%, Ti: 0.06 wt.%, Al: balance. The Carbon Fabric/Polypropylene prepreg was used as a Skin Material

2.2 Preparation of the Sandwich Specimen

Aluminium alloy Foam was made through melt foaming method by stir casting technique. Firstly, the alloy was melt at a temperature of 700-750 ℃. Then, preheated (1000 ℃ for 3 hrs) melt is Stirred by using mechanical stirring at a speed 800 rpm. stirring was continued for 2-3 minutes to ensure its complete and homogeneous mixing. Finally, dry CaH2 particles (of average size: 18μm ± 3μm at 0.6 wt.%) were added manually in the melt again through mechanical stirring. The melt temperature was varied (640 to 670 ºC) to obtain varying ρ_{rd}. The temperature was maintained for another two minutes after addition of CaH_2 for complete foaming. Finally, the crucible with liquid foam cooled fast by steam spraying to get Aluminium Foam.

Materials were cut down to a size of 200 × 200 mm, with the aluminium foam cut using a band saw. The sandwich structures were made by placing a single ply of the Carbon fibre/polypropylene prepreg on either side of the aluminium foam core in a picture frame mould. Two layers of a 50μm thick hot-melt polypropylene-based adhesive were placed at each bi-material interface. This method has been found to provide good bonding between the foam and the thermoplastic skin.

The mould was heated to 185ºC in a heated platen press, using a thermocouple within the Twintex layer to monitor the thermoplastic temperature. The structure was then held at a pressure of 2.5 MPa while it was rapidly water cooled to consolidate the skin material. Variations in the process included altering the core thickness or using an increased number of plys of skin prepreg material. The consolidated sandwich panels with core thicknesses of 10 mm, and a single ply skin had average thicknesses of 5 mm. The apparent increase in skin thickness for the single ply skin as the core thickness increases may be related to the increase in cell diameter. During the sandwich manufacturing process, the thermoplastic matrix material may experience some flow while in the liquid state before consolidation. This may result in some matrix material moving into the cells of the aluminium foam, particularly in the core with the larger cell size, reducing the overall thickness of the skin. Samples for testing were cut to width from the panels using a diamond tipped saw.

2.3 Micrograph

To obtain optical images of specimens, a Nikon D7000 DSLR camera equipped with an AF-S VR Micro-Nikkor 105 mm f/2.8G IF-ED macro lens was used. Optical microscopy was conducted using a Nikon Epiphot 200 microscope fitted with a Nikon DS-Fil digital camera. The specimen preparation was conducted using standard metallographic procedures including grinding and polishing down to 1 μm slurry and etching using a solution of one-part nitric acid in 20 parts alcohol.

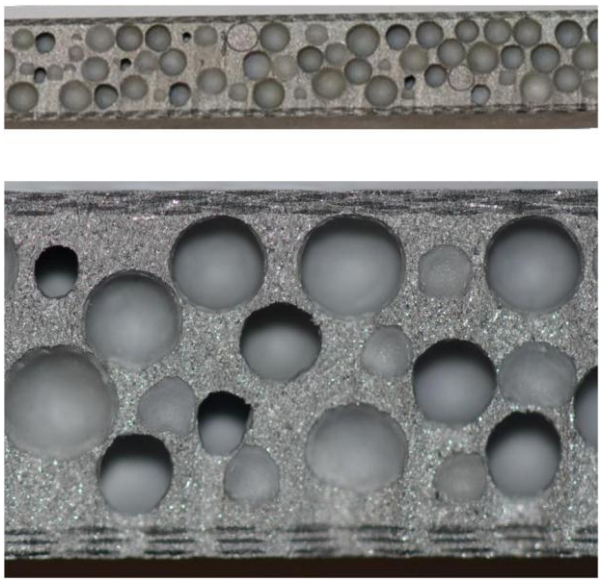

Fig.1 Aluminium Foam Sandwich Composites with Carbon Face Sheet

2.4 Dynamic Modal Analysis

The scope of these experiments is to characterize the material by performing a dynamic modal analysis. The focus is on the Young's modulus and the damping parameter tan δ. The storage modulus E' and the loss modulus E'' are also investigated. The storage and loss moduli are related to the Young's modulus by

$$E = \sqrt{E'^2 + E''^2} \quad (1)$$

It is possible to express the storage modulus as a measure of the energy stored in the material during deformation. The loss modulus is a measure of the energy dissipated per loading cycle. The tan δ is obtained by the ratio of loss and storage moduli and represents the lag between the response of the stress and the strain due to the applied load. The PSD measurement provides the beam deflection $y(\tau)$ by

$$y(\tau) = h(x_1, \tau) \quad (2)$$

Where τ is the time. The deflection is given by

$$h(x, \tau) = \sum_{n=1}^{N} X_n(\tau) \emptyset_n(x) \quad (3)$$

Where $X_n(\tau)$ is the nth modal coefficient and $\emptyset_n(x)$ is the nth mode function for the cantilever computed according to [34].

$$\emptyset_n(x) = \sin\left(\frac{\lambda_n x}{e}\right) - sinh\left(\frac{\lambda_n x}{e}\right) - \frac{\sin(\lambda_n)+\sin h(\lambda_n)}{cos(\lambda_n)+cos(\lambda_n)}\left[\cos\left(\frac{\lambda_n x}{e}\right) - cosh\left(\frac{\lambda_n x}{e}\right)\right] \quad (4)$$

Where e is the beam free length and $\lambda_1 = 1.875, \lambda_2 = 4.694, \lambda_3 = 7.855$ are the first three solutions of the transcendental equation

$$\cos(\lambda e)\, cosh(\lambda e) = -1 \quad (5)$$

The deflection of the beam is observed at the 1st iteration and the results are plotted in Fig. 6. The Fast Fourier Transform of $X_n = a_1$ is then performed. The magnitude of the 1st modal coefficient allows computing the phase of the signal by acquiring the relative bin number. The resolution of the frequency response is 2.4 Hz.

The governing equation of motion for the specimen vibration in the Fourier domain, neglecting air damping, can be written according to [23].

$$E^*(\omega)\frac{I\partial^4\tilde{h}(x,\omega)}{\partial x^4} - \rho A\omega^2\tilde{h}(x,\omega) = P\psi(x - x_2) \quad (6)$$

Where $E^*(\omega)$ is the complex Young's modulus, I is the cross-section moment of inertia with respect to the centroidal axis orthogonal to the vibration plane, ρ is the mass density, A is the area of the cross section, ψ is the Dirac delta generalized function, and $P\psi(x - x_{2)}$ is the load applied by the impact hammer. Projecting Eq. (6) on the mode shapes set

$$\int_0^l E^*(\omega)\beta_n^4 X_n(x)X_n(x)\widetilde{\varphi_n}(\omega)dx - \int_0^l \rho A\omega^2\widetilde{\varphi_n}(\omega)X_n(x)X_n(x)dx = \int_0^l P\psi(\mathrm{x} - x_2)X_n(x)dx \quad (7)$$

Taking $X_n(x)X_n(x) = 1$ and $\psi(x - x_2)X_n(x) = PX_n(x_2)$ provides

$$E^*(\omega)I\beta_n^4\widetilde{\varphi_n}(\omega) - \rho A\omega^2\widetilde{\varphi_n}(\omega) = PX_n(x_2) \quad (8)$$

For moderately low values of structural damping, in the proximity of the mth resonance frequency, the system can be modelled with a single degree of freedom and the Young's modulus can be assumed to be constant over the frequency range. The resonance frequency is given by

$$\omega_m^2 = \frac{E'(\omega_m)I\beta_n^4}{\rho A} \quad (9)$$

Since the Young's modulus can be assumed constant, especially for narrow frequency ranges, it can be computed by Refs. [35-37].

$$E = \left(\frac{M}{L}\right)\left(\frac{12}{bt^3}\right)(2\pi f_n)^2\left(\frac{l^2}{\beta_n^2 l^2}\right)^2 \quad (10)$$

where M is the total mass of the beam, L is the total length of the beam, b is the width of the beam, t is the thickness of the beam, f_n is the n-th mode of the natural frequency, l is the free length of the beam and $\beta_n l$ is the value corresponding to the n-th mode of the natural frequency.

During the study of a three-layered skin sandwich beam [38], used the damping ratio ζ to approximate the loss factor. They consider $\tan(\delta) = \zeta$, where ζ is computed by

$$\tan(\delta) = \zeta = \frac{\log\left(\frac{x_1}{x_n}\right)}{2n\pi} \quad (11)$$

Since $\tan(\delta) = \frac{E''}{E'}$, the loss modulus E'' is

$$E'' = \tan(\delta)E' \quad (12)$$

For small damping ratios, the damping in the material can be incorporated into a complex modulus [36]:

$$E^* = E'(1 + 2i\zeta) \quad (13)$$

2.5 Experimental Setup

A specimen clamp is assembled by using two aluminium blocks with dimensions 101 x 101 x 19 mm^3. The bottom block is bolted to a Newport ST Series optical table with IQ Damping Technology and the top block is anchored to the bottom block. A torque of 15 Nm is applied to the screws holding the two blocks to minimize friction damping. The higher stiffness and considerably larger size of the aluminium blocks with respect to the test specimen minimizes structural perturbations. A LMI LSD Laser Distance Sensor 80/10 is used for amplitude measurement. This triangulation principle based laser does not need mirrors mounted on the specimen surface so there is no added mass for the beam. The laser system works with a position sensing detector (PSD) sensor installed inside the same equipment assembly. A position sensing detector is a semiconductor device, which gives electrical output based on the position of the light spot falling on the surface of the device [33].

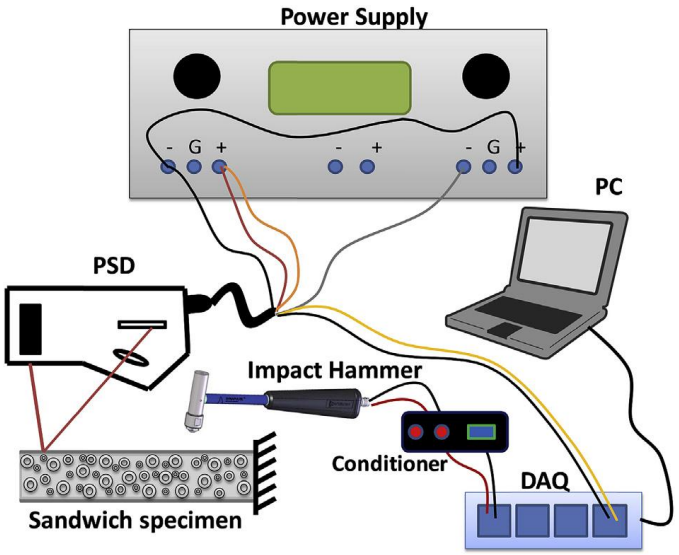

Fig. 2. Schematic of the experimental setup for vibration testing of the sandwich specimens.

The LDS 80/10 measurement range is 10 mm, the offset distance (OD) is 75 mm, the typical resolution is 0.001 mm,

and the acquisition frequency is 3 kHz. The sensor is linear with an output of 0-10 Vdc with 1 V/mm. The laser requires a ±15 V DC power supply and to obtain the required voltage levels; a BK Precision 1672 Triple Output DC power supply is used. A schematic of the setup is shown in **Fig. 2 & 3.** The signal cables of the impact hammer and laser are connected to the data acquisition board (National Instruments DAQ). The board is connected to a computer and the signals are acquired by using LabView 2012 SP1 (32bit) software.

A Bruel & Kjaer Impact Hammer, Type 8204, 22 mV/N, is used to excite the beam. It is connected to an Endeveco conditioner, model 4416B. The gathered signals are Fourier transformed by using a MATLAB R2013b routine to obtain the system transfer function, which is used to identify the storage modulus and the loss tangent. Three specimens for each type of composite are tested. Each specimen is tested for three different free lengths in order to cover a wide frequency range. For each length three repetitions are performed.

Fig. 3. experimental setup for vibration testing of the sandwich specimens with Data acquisition System

2.6 Results

2.6.1 *Vibration Test Results*

Three specimens of S1 and three specimens S3 sandwich were tested for three different free lengths of 0.095 m, 0.1m and 0.105m, and each length was tested three times. In each single test the specimen was hit three times with the impact hammer. **Fig. 4** presents the impact hammer and position sensing detector outputs. The oscillation frequency of the specimen is shown in **Fig. 5**. The resonant frequency, storage modulus and tan δ were obtained through the MATLAB code. The mean and standard deviation values for the S1 and S3 specimens are provided in **Table 4**. The S3 sandwich exhibited 13% higher storage modulus than the S1 sandwich, which is attributed to the three layers of skin that provide increased stiffness to the S3 specimen. The increased stiffness is achieved at the expense of damping and the damping ratio is higher in the S1 sandwich by 11.5%. A longer specimen could help in reducing the noise by increasing the amplitude. As shown in literature the damping ratio exhibits both frequency and amplitude dependence [36]. Equation (1) presents the relation between Young's modulus and storage and loss moduli. In the strict sense the Young's modulus presented by this equation is a complex quantity. However, the ratio of storage to loss moduli is on the order of 10^3 for the stiff sandwich beams tested in this work. In this case, the loss modulus can be neglected to consider storage modulus to be the Young's modulus of the material.

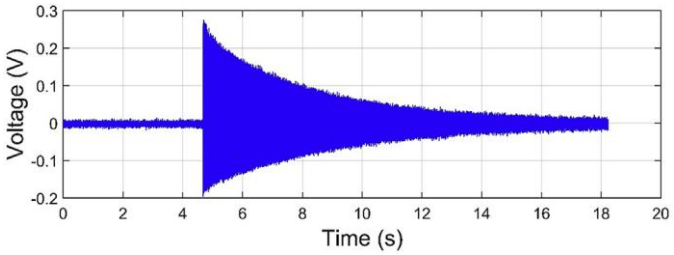

Figure 4: Position Sensor Detector Output

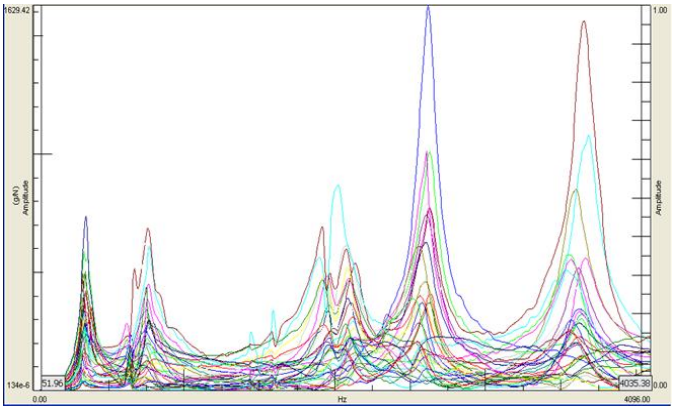

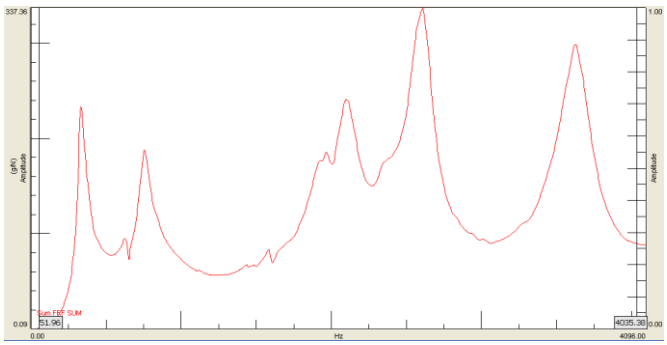

Figure 5: Oscillation Frequency of the Specimen

Table 1: Mean and standard deviation values of properties obtained for the metal matrix syntactic foam core sandwich composite.

Sandwich Type	Nomenclature	$E'\ (GPa)$	$\tan(\delta)$	$E''\ (GPa)$	$E\ (GPa)$
One layer skin	S1	32.57 ± 2.15	0.0052 ± 0.0036	0.169	32.57
Three layer skin	S2	37.33 ± 1.12	0.0046 ± 0.0036	0.171	37.33

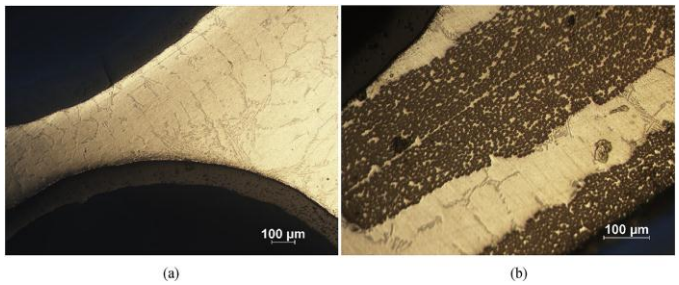

Figure-6: (a) Optical micrograph shows the matrix region between three alumina hollow particles, **(b)** optical micrograph showing the matrix microstructure

Optical micrographs presented in Fig. 6(a) show a continuous interface between particles and matrix, which indicates that the particles are wetted by the matrix and there are no interfacial defects. In addition, the fabric tows are also found to be completely penetrated by the matrix as observed in Fig. 6(b). Detailed microscopic observations on these sandwich composites are available in previous studies [19,20].

2.7 Conclusions

- The present work was focused on studying syntactic foam core sandwich composites for vibration response. The sandwich core consisted of Al 2014 alloy filled with alumina particles, and the external skins were made of one or three layers of $0^0/90^0$ carbon fabric sheets. The material is characterized by using the vibration response. The main conclusions can be summarized as follows:
- The sandwich has storage modulus of 32.57 ± 2.15 GPa for the single layer configuration and 37.33 ± 1.12 GPa for the three-layer skin configuration. The difference between the two samples is 13%. This difference is due to the increased stiffness provided by the carbon fabric sheets. The outcomes of the theoretical computations showed a Young's modulus of 27.8 GPa and 103.6 GPa for the core and the external skin composite materials, respectively.
- The damping ratios were 0.0052 ± 0.0036 for the single layer carbon fabric sandwich and 0.0046 ± 0.0036 for the three-layer sandwich. The difference is 11.5%.
- The experimental results obtained are in agreement with the theoretical computations for the composite sandwich material. The theoretical results have provided a value of 31.2 and 38.1 GPa for the single and the three layered sandwich Young's modulus. The differences with the experimental values are 4.2% and 2.0% respectively.
- As the loss modulus is three orders of magnitude smaller than the storage modulus, the storage modulus is taken as the estimate of the Young's modulus.

REFERENCES

[1] J.A. Santa Maria, B.F. Schultz, J. Ferguson, N. Gupta, P.K. Rohatgi, Effect of hollow sphere size and size distribution on the quasi-static and high strain rate compressive properties of Al-A380-Al2O3 syntactic foams, J. Mater. Sci. 49 (3) (2014) 1267-1278.

[2] I.N. Orbulov, J. Ginsztler, Compressive characteristics of metal matrix syntactic foams, Compos. Part A Appl. Sci. Manuf. 43 (4) (2012) 553-561.

[3] V.C. Shunmugasamy, D. Pinisetty, N. Gupta, Viscoelastic properties of hollow glass particle filled vinyl ester matrix syntactic foams: effect of temperature and loading frequency, J. Mater. Sci. 48 (4) (2013) 1685-1701.

[4] A. Macke, B.F. Schultz, P.K. Rohatgi, N. Gupta, Metal matrix composites for automotive applications, Adv. Compos. Mater. Automot. Appl. Struct. Integr. Crashworthiness (2013) 311-344.

[5] X. Tao, Y. Zhao, Compressive failure of Al alloy matrix syntactic foams manufactured by melt infiltration, Mater. Sci. Eng. A 549 (2012) 228-232.

[6] D.K. Balch, D.C. Dunand, Load partitioning in aluminium syntactic foams containing ceramic microspheres, Acta Mater. 54 (6) (2006) 1501-1511.

[7] J.-M. Berthelot, Y. Sefrani, Damping analysis of unidirectional glass and Kevlar fibre composites, Comp. Sci. Technol. 64 (9) (2004) 1261-1278.

[8] K. Maslov, V.K. Kinra, Amplitudeefrequency dependence of damping properties of carbon foams, J. Sound Vib. 282 (3) (2005) 769-780.

[9] R. Pal, Modeling viscoelastic behavior of particulate composites with high volume fraction of filler, Mater. Sci. Eng. A 412 (1) (2005) 71-77.

[10] J.H. Yim, J. Gillespie Jr., Damping characteristics of 0 and 90 AS4/3501-6 unidirectional laminates including the transverse shear effect, Compos. Struct. 50 (3) (2000) 217-225.

[11] X. Tao, Y. Zhao, Compressive behavior of Al matrix syntactic foams toughened with Al particles, Scr. Mater. 61 (5) (2009) 461-464.

[12] D.K. Balch, J.G. O'Dwyer, G.R. Davis, C.M. Cady, G.T. Gray, D.C. Dunand, Plasticity and damage in aluminium syntactic foams deformed under dynamic and quasi-static conditions, Mater. Sci. Eng. A 391 (1) (2005) 408-417.

[13] I.N. Orbulov, J. Dobr_anszky, Producing metal matrix syntactic foams by pressure infiltration, Period. Polytech. Eng. Mech. Eng. 52 (1) (2008) 35.

[14] L. Licitra, D.D. Luong, O.M. Strbik III, N. Gupta, Dynamic properties of alumina hollow particle filled aluminium alloy A356 matrix syntactic foams, Mater. Des. 66 (2015) 504-515.

[15] J. Cox, D.D. Luong, V.C. Shunmugasamy, N. Gupta, O.M. Strbik III, K. Cho, Dynamic and thermal properties of aluminium alloy A356/silicon carbide

hollow particle syntactic foams, Metals 4 (4) (2014) 530-548.

[16] D.D. Luong, O.M. Strbik III, V.H. Hammond, N. Gupta, K. Cho, Development of high performance lightweight aluminium alloy/SiC hollow sphere syntactic foams and compressive characterization at quasi-static and high strain rates, J. Alloys Compd. 550 (2013) 412-422.

[17] L. Wan, Y. Huang, S. Lv, J. Feng, Fabrication and interfacial characterization of aluminium foam sandwich via fluxless soldering with surface abrasion, Compos. Struct. 123 (2015) 366-373.

[18] M. Jackson, A. Shukla, Performance of sandwich composites subjected to sequential impact and air blast loading, Compos. Part B Eng. 42 (2) (2011) 155-166.

[19] M.Y. Omar, C. Xiang, N. Gupta, O.M. Strbik III, K. Cho, Syntactic foam core metal matrix sandwich composite: compressive properties and strain rate effects, Mater. Sci. Eng. A 643 (2015) 156-168.

[20] M.Y. Omar, C. Xiang, N. Gupta, O.M. Strbik III, K. Cho, Syntactic foam core metal matrix sandwich composite under bending conditions, Mater. Des. 86 (2015) 536-544.

[21] M.Y. Omar, C. Xiang, N. Gupta, O.M. Strbik III, K. Cho, Data characterizing compressive properties of Al/Al2O3 syntactic foam core metal matrix sandwich, Data Brief 5 (2015) 522-527.

[22] M.Y. Omar, C. Xiang, N. Gupta, O.M. Strbik III, K. Cho, Data characterizing flexural properties of Al/Al2O3 syntactic foam core metal matrix sandwich, Data Brief 5 (2015) 564-571.

[23] G. Tagliavia, M. Porfiri, N. Gupta, Vinyl ester-glass hollow particle composites: dynamic mechanical properties at high inclusion volume fraction, J. Compos. Mater. 43 (5) (2009) 561-582.

[24] R.F. Gibson, Modal vibration response measurements for characterization of composite materials and structures, Compos. Sci. Technol. 60 (15) (2000) 2769-2780.

[25] L. Hillstrom, M. Mossberg, B. Lundberg, Identification of complex modulus from measured strains on an axially impacted bar using least squares, J. Sound Vib. 230 (3) (2000) 689-707.

[26] K. Mahata, T. Soderstrom, Bayesian approaches for identification of the complex modulus of viscoelastic materials, Automatica 43 (8) (2007) 1369-1376.

[27] K. Pradhan, S. Chakraverty, Free vibration of Euler and Timoshenko functionally graded beams by Rayleigh-Ritz method, Compos. Part B Eng. 51 (2013) 175-184.

[28] S. Chonan, Vibration and stability of sandwich beams with elastic bonding, J. Sound Vib. 85 (4) (1982) 525-537.

[29] V.S. Sokolinsky, H.F. Von Bremen, J.A. Lavoie, S.R. Nutt, Analytical and experimental study of free vibration response of soft-core sandwich beams, J. Sandw. Struct. Mater. 6 (3) (2004) 239-261.

[30] R. Ni, R. Adams, The damping and dynamic moduli of symmetric laminated composite beams-theoretical and experimental results, J. Compos. Mater. 18 (2) (1984) 104-121.

[31] M. Assarar, A. El Mahi, J.-M. Berthelot, Analysis of the damping of sandwich materials and effect of the characteristics of the constituents, Int. J. Mater. Sci. 3 (2) (2013) 61-71.

[32] D.S. Prasad, A.R. Krishna, Tribological properties of A356. 2/RHA composites, J. Mater. Sci. Technol. 28 (4) (2012) 367-372.

[33] S. Kouno, PSD sensor decomposing multiple light spots, J. Robot. Mechatron. 18 (1) (2006) 97.

[34] S. Timoshenko, D. Young, W. Weaver Jr., Vibration Problems in Engineering, John Wiley & Sons, 1974.

[35] E.M. Priest, Free Vibration Response Comparison of Composite Beams with Fluid Structure Interaction, 2012 (DTIC Document).

[36] A.B. Schultz, S.W. Tsai, Dynamic moduli and damping ratios in fiber-reinforced composites, J. Compos. Mater. 2 (3) (1968) 368-379.

[37] M. Assarar, A. El Mahi, J.-M. Berthelot, Damping analysis of sandwich composite materials, J. Compos. Mater. 43 (13) (2009) 1461-1485.

[38] N. Barbieri, R. Barbieri, L.C. Winikes, L.F. Oresten, Estimation of parameters of a three-layered sandwich beam, J. Mech. Mater. Struct. 3 (3) (2008) 527-544.

[39] H. Ledbetter, M.L. Dunn, Equivalence of Eshelby inclusion theory and Wech-sler-Lieberman-Read, Bowles-mackenzie martensite-crystallography theories, Mater. Sci. Eng. A 285 (1) (2000) 180-185.

[40] A. Johnson, G. Sims, Mechanical properties and design of sandwich materials, Composites 17 (4) (1986) 321-328.

[41] D.F. O'Regan, B. Meenan, A comparison of Young's modulus predictions in fibre-reinforced-polyamide injection mouldings, Compos. Sci. Technol. 59 (3) (1999) 419-427.

[42] E.F. Crawley, M.C. Van Schoor, Material damping in aluminium and metal matrix composites, J. Compos. Mater. 21 (6) (1987) 553-568. [6] Licitra, L., D.D. Luong, O.M. Strbik III, and N. Gupta, Dynamic properties of alumina hollow particle filled aluminium alloy A356 matrix syntactic foams. Materials & Design, 2015. 66, Part B: p. 504-515.